Digestive Diseases and Sciences (2022) 67:504–515
https://doi.org/10.1007/s10620-021-06859-w

ORIGINAL ARTICLE

Knockdown of circRAD23B Exerts Antitumor Response in Colorectal Cancer via the Regulation of miR-1205/TRIM44 axis

Bingbing Han[1] · Xiaohong Wang[2] · Xia Yin[3]

Received: 4 August 2020 / Accepted: 18 January 2021 / Published online: 25 February 2021

Abstract

Background Colorectal cancer (CRC) is a common cancer with high metastatic property. Circular RNAs (circRNAs) have important involvement in cancer processes. This study focused on the regulation of circRNA RAD23 homologue B (circRAD23B) in CRC.

Methods The levels of circRAD23B, microRNA-1205 (miR-1205), and tripartite motif-44 (TRIM44) were examined by quantitative real-time polymerase chain reaction (qRT-PCR). Functional analyses were performed by Cell Counting Kit-8 (CCK-8) for cell proliferation, flow cytometry for cell cycle or cell apoptosis, and transwell assay for cell migration and invasion. Western blot was administrated for protein detection. The interaction of targets was analyzed by dual-luciferase reporter and RNA pull-down assays. The in vivo experiment was conducted via xenograft tumor in mice.

Results We identified that circRAD23B was overexpressed in CRC tissues and cells. CRC cell proliferation, cell cycle progression, and cell metastasis were inhibited, while apoptosis was promoted by downregulating circRAD23B. Target analysis indicated that circRAD23B-targeted miR-1205 and TRIM44 were downstream genes of miR-1205. Moreover, the antitumor response of circRAD23B downregulation and miR-1205 overexpression was, respectively, achieved by increasing miR-1205 and decreasing TRIM44. CircRAD23B could regulate TRIM44 level by sponging miR-1205. In vivo, circRAD23B knockdown also reduced CRC tumorigenesis via the miR-1205/TRIM44 axis.

Conclusion These results suggested that the inhibition of circRAD23B retarded the progression of CRC via acting on the miR-1205/TRIM44 axis. CircRAD23B might be a novel target in CRC treatment.

Keywords circRAD23B · Colorectal cancer · miR-1205 · TRIM44

Introduction

Colorectal cancer (CRC) is an aggressive disease with enormous challenges in diagnostic and therapeutic optimization to reduce mortality in the clinic [1]. Molecular diagnostics with high accuracy and sensitivity have been developed as effective tools in screening and diagnosing CRC [2]. In addition, some cellular biomolecules were reported to monitor the therapeutic process for CRC [3]. To seek novel targets used for the diagnosis and treatment of CRC is quite necessary.

Circular RNAs (circRNAs) are a novel family of endogenous noncoding RNAs (ncRNAs) with ubiquitous expression in eukaryotes and can affect various cancer cellular phenotypes [4]. CircRNAs play as functional microRNA (miRNA) sponges to regulate the expression of downstream genes [5]. Lu et al. reported that silencing of circ-FARSA suppressed CRC cell growth and metastasis by inhibiting the miR-330-5p-mediated LASP1 expression [6]. Circ_0007142 promoted CDC25A to induce CRC malignance via sponging miR-122-5p [7], and hsa_circ_0008285 was a tumor-inhibitory factor in CRC via the regulation of miR-382-5p/PTEN axis [8].

CircRNA RAD23 homologue B (circRAD23B) has been identified as an oncogene in lung cancer [9] and esophageal cancer [10]. Han et al. found that circRAD23B enhanced

✉ Xia Yin
muvrnz@163.com

[1] Department of Gastroenterology, Weifang No.2 People's Hospital, Weifang, Shandong, China

[2] Department of Health, Weifang No.2 People's Hospital, Weifang, Shandong, China

[3] Department of Neurology, Weifang No.2 People's Hospital, No.7 Yuanxiao Street, Kuiwen District 261042, Weifang, Shandong, China

cell growth and invasion in nonsmall cell lung cancer via the miR-593-3p/CCND2 or miR-653-5p/TIAM1 signal axis [11]. However, circRAD23B is an unexplored circRNA in CRC. Previous studies have suggested that microRNA-1205 (miR-1205) played an inhibitory role in epithelial-to-mesenchymal transition (EMT) of CRC cells [12] and tripartite motif-44 (TRIM44) served for a cancer-promoting gene in CRC [13, 14].

In this study, the functional investigation of circRAD23B in CRC will be performed. Moreover, we put forward the hypothesis that circRAD23B acted as a miR-1205 sponge to regulate TRIM44 in CCRC and affirmed it by performing a series of experiments.

Materials and Methods

Acquisition of Human Samples

The current study was approved by the Ethics Review Committee of Weifang No.2 People's Hospital, and all protocols strictly followed the Declaration of Helsinki involving human subjects. After surgical resection of CRC patients at Weifang No.2 People's Hospital, we have collected 50 paired CRC and the corresponding normal tissues (away from cancer tissues for more than 2 cm). These human samples were snap-frozen in liquid nitrogen and then preserved at − 80 °C. Fifty patients have provided written informed consent before surgery. The inclusion criteria of patients were shown as below: (1) patients were diagnosed as CRC after pathological examination; (2) patients have not received radiotherapy or chemotherapy prior to the surgery; and (3) patients were voluntarily involved in this study. The clinicopathologic features of patients are presented in Table 1.

Table 1 Correlation between clinicopathologic features and circRAD23B expression in the colorectal cancer cases

Variables	No. of cases	CircRAD23B expression		*P*-value
		High (n = 25)	Low (n = 25)	
Gender				0.370
Male	33	15	18	
Female	17	10	7	
Ages				0.758
< 45	15	8	7	
≥ 45	35	17	18	
Tumor size (cm)				0.089
< 5	26	10	16	
≥ 5	24	15	9	
TNM stage				0.004*
I–II	37	14	23	
III	13	11	2	
Metastatic status				0.023*
Yes	22	15	7	
No	28	10	18	

*$P < 0.05$

Cell Culture

Human normal enterocyte NCM460 (QCB309; QCHENG BIO, Shanghai, China) was maintained in Dulbecco's modified eagle medium (DMEM; Hyclone, Logan, UT, USA). CRC cell lines SW480 (CCL-228) and SW620 (CCL-227) were purchased from American Type Culture Collection (ATCC, Manassas, VA, USA) and sustained in L-15 medium (Hyclone). 10% fetal bovine serum (FBS; Sigma-Aldrich, St. Louis, MO, USA) and 1% penicillin–streptomycin solution (Millipore, Billerica, MA, USA) were complemented for great cell growth. Cells were cultured under the conditions of 5% CO_2 at 37 °C.

Oligonucleotides or Vectors Transfection

After cell seeding overnight to 70% confluence, oligonucleotides or vectors were transfected into SW480 and SW620 cells by Lipofectamine™ 3000 Transfection Reagent (Invitrogen, Carlsbad, CA, USA). The oligonucleotides were directly bought from RIBOBIO (Guangzhou, China): small interfering RNAs (siRNAs) targeting circRAD23B (si-circRAD23B#1, si-circRAD23B#2, si-circRAD23B#3), miR-1205 mimic and inhibitor (miR-1205 and anti-miR-1205), and the matched negative controls (si-NC, miR-NC, and anti-miR-NC). For the overexpression of circRAD23B and TRIM44, their sequences were, respectively, cloned into pcircRNA 2.2 hsa vector (pcirc; BersinBio, Guangzhou, China) and pcDNA vector (Invitrogen) to obtain the recombinant vectors circRAD23B and TRIM44.

RNA Isolation, Treatment, and the Quantitative Real-Time Polymerase Chain Reaction (qRT-PCR)

TRI reagent (Sigma-Aldrich) was used for processing tissues and cells to acquire total RNA. For RNase R treatment, 2 μg RNA was added with 6 U RNase R (Epicentre Technologies, Madison, WI, USA) at 37 °C for 1 h. The complementary DNA (cDNA) was synthesized using cDNA Synthesis Supermix (Bio-Rad, Hercules, CA, USA), and then the qRT-PCR was performed by iTaq Universal SYBR Green Supermix (Bio-Rad) on the CFX96 Dx Real-Time PCR System (Bio-Rad). Glyceraldehyde phosphate dehydrogenase (GAPDH) and U6 served as the housekeeping genes in this study, respectively, for circRNA/mRNA and miRNA. The $2^{-\Delta\Delta Ct}$ method was used to analyze the relative levels of

genes. Primers sequences of forward (F) and reverse (R) were as follows: circRAD23B, 5′-GCAAGTAATTGCAGCCCTGAG-3′ (F) and 5′-GCTGAGTTGTAGCTGGTGCT-3′ (R); RAD23B, 5′-CTTCCTCCACCACCACAACT-3′ (F) and 5′-GGTGTCTCTGCTGGCTTTTC-3′ (R); miR-1205, 5′-CTGCAGGGTTTGCTTTGAGG-3′ (F) and 5′-CTCCAGAACAGGGTTGACAGG-3′ (R); TRIM44, 5′-GTGGACATCCAAGAGGCAAT-3′ (F) and 5′-AGCAAGCCTTCATGTGTCCT-3′ (R); GAPDH, 5′-CTCTGCTCCTCCTGTTCGAC-3′ (F) and 5′-GCGCCCAATACGACCAAATC-3′ (R); and U6, 5′-GCTTCGGCAGCACATATACTAAAAT-3′ (F) and 5′-CGCTTCACGAATTTGCGTGTCAT-3′ (R).

Cell Proliferation Assay

1×10^4 SW480 and SW620 cells were suspended in 100 μL L-15 medium and then transplanted into the 96-well plates. After 24-h culture, cell transfection was performed for 0 h, 24 h, 48 h, and 72 h, respectively. 10 μL/well CCK-8 solution (Nanjing Jiancheng Bioengineering Institute, Nanjing, China) was added into the wells with no bubble. The absorbance at the wavelength of 450 nm was detected via a microplate reader (Bio-Rad) 3 h later.

Cell Apoptosis Detection

Apoptotic generation in cells was determined using Annexin V-FITC/PI double-staining apoptosis detection kit (Nanjing Jiancheng Bioengineering Institute) by flow cytometry. In brief, cells were harvested through the digestion of trypsin (Sigma-Aldrich) after 72-h transfection. Then, cells were resuspended in phosphate buffer solution (PBS; Hyclone) and 3×10^5 cell pellets were mixed with 500 μL 1 × binding buffer. After the addition of 5 μL Annexin V-FITC and 5 μL propidium iodide (PI) for 10 min in the dark, cell detection was instantly conducted under the flow cytometer (BD Biosciences, San Diego, CA, USA) with Annexin V-FITC as green fluorescence and PI as red fluorescence. The apoptotic cells indicated those cells stained by Annexin V-FITC (+)/PI(−) and Annexin V-FITC(+)/PI(+).

Cell Cycle Analysis

Cell cycle proportion was examined via Cell cycle detection kit (Nanjing Jiancheng Bioengineering Institute) by flow cytometry. 5×10^5 collected cells were suspended in 300 μL PBS (Hyclone), and then cell suspension was added to 1.2 mL ice-cold ethanol (Sigma-Aldrich) at − 20 °C overnight. Thereafter, cells were centrifuged at 2000 rpm for 5 min and washed with 1 mL PBS, followed by the resuspension in 100 μL RNase A solution at 37 °C for 30 min. Four hundred microliters of PI was then mixed with cells at 4 °C for 30 min away from light, and the absorbance at 488 nm was read by a flow cytometer (BD Biosciences).

Cell Migration and Invasion Examination

Cell migration and invasion were examined in transwell chamber (Corning Inc., Corning, NY, USA) and transwell chamber precoated with matrigel (Corning Inc.). The upper chamber was added with transfected cells in serum-free medium, and the complete medium was added into the lower chamber. After cell seeding for 24 h, cells on the lower surface of the polycarbonate membrane were fixated in 4% paraformaldehyde (Sigma-Aldrich) and stained by crystal violet (Sigma-Aldrich). Cell image acquisition (100 × magnification) and cell counting were performed under an inverted microscope (Olympus, Tokyo, Japan).

Western Blot

Total proteins were rapidly and efficiently isolated from CRC tissues and cells applying with RIPA Buffer (Sigma-Aldrich). The protein levels of different genes were detected referring to the previous study [15] using the following antibody: anti-matrix metalloproteinase 2 (anti-MMP2; Abcam, Cambridge, UK, ab97779, 1:1000), anti-MMP9 (Abcam, ab38898, 1:1000) and internal control GAPDH (Abcam, ab9485, 1:3000). After the incubation of Goat Anti-Rabbit IgG H&L (HRP) (Abcam, ab205718, 1:5000), the protein bands were presented via the coloration by ECL Western Blotting Substrate Kit (Abcam). Ultimately, the protein quantification was performed using Labworks™ Analysis Software version 4.0 (Labworks, Upland, CA, USA).

Dual-Luciferase Reporter Assay

The luciferase reporter plasmids of wild-type (WT) and mutant-type (MUT) circRAD23B (circRAD23B WT and circRAD23B MUT) or TRIM44 (TRIM44 3′UTR WT and TRIM44 3′UTR MUT) were constructed using the basic luciferase vector pGL-3 control (Promega, Madison, WI, USA). At 48 h after cotransfection of circRAD23B WT/circRAD23B MUT/TRIM44 3′UTR WT/TRIM44 3′UTR MUT and miR-1205/miR-NC, SW480 and SW620 cells were collected and the relative luciferase intensity was measured by the Dual-Luciferase Reporter Assay System (Promega) as per the guidance for users.

Pull-Down Assay with Biotinylated miR-1205

To analyze the binding between miR-1205 and TRIM44, Biotin-coupled miR-1205 (Bio-miR-1205) and negative control Bio-miR-NC were, respectively, transfected into SW480 and SW620 cells. Cell lysates were then incubated

in Streptavidin Magnetic Beads (Thermo Fisher Scientific, Waltham, MA, USA), and the RNA complexes were extracted. Employing the cDNA as the amplified templates, TRIM44 mRNA expression was assayed using qRT-PCR as mentioned above.

Xenograft Tumor Assay

Six-week-old male BALB/c nude mice were purchased from Shanghai SIPPR-BK Laboratory Animal Co. Ltd. (Shanghai, China). Mice were cared in the specific pathogen-free (SPF) environment with a constant temperature of 26 °C, a humidity of 70%, and a programmed cycle (12-h light/12-h dark) for circadian control. 5×10^6 transfected SW480 cells were suspended in 200 μL PBS, and the prepared cell suspension was subcutaneously injected into the flanks of mice, with five mice in sh-NC or sh-circRAD23B group. Every 7 days after cell injection, tumor size was evaluated by the length (L) and weight (W), followed by the calculation of tumor volume using the standard formula: $L \times W^2 \times 0.5$. Tumors were isolated from killed mice after 28 days, and tumors were weighed. The genic detection was carried out by qRT-PCR and western blot after purification of RNA and protein. All mice were painlessly killed by CO_2 asphyxia method (using CO_2 to replace the air of container with 30% of volume/min), and the killed mice were buried after tissue collection. This animal assay was empowered by Animal Ethics Committee of Weifang No.2 People's Hospital, and the experiments on mice were implemented strictly according to the principles for the Care and Use of Laboratory Animals of National Institute of Health.

Statistical Analysis

In this study, data expressed as the mean ± standard deviation (SD) were statistically analyzed via SPSS 20.0 (SPSS Inc., Chicago, IL, USA). Student's t test was applied for the comparison between two groups, and difference analyses among multiple groups were administrated via one-way analysis of variance (ANOVA) followed by Tukey's test. The difference was significant when $P < 0.05$.

Results

CircRAD23B Was Highly Expressed in CRC Tissues and Cells

Gene Expression Omnibus (GEO) dataset GSE126094 (https://www.ncbi.nlm.nih.gov/geo/geo2r/?acc=GSE126094) indicated that circRAD23B was upregulated in human CRC samples compared with Normal samples (Fig. 1a). According to the cutoff criteria of values of |log2 fold change| (|log2FC|) > 1 and $P < 0.05$, there were many dysregulated circRNAs (1831 upregulated and 20 downregulated) in the GSE126094 dataset (Fig. 1b). CircRAD23B is one of the upregulated circRNAs derived from the Exon4-6 of RAD23B gene with the closed-loop structure (Fig. 1c). The upregulation of circRAD23B was also found in our collected CRC tissues and cultured cells (SW480 and SW620)

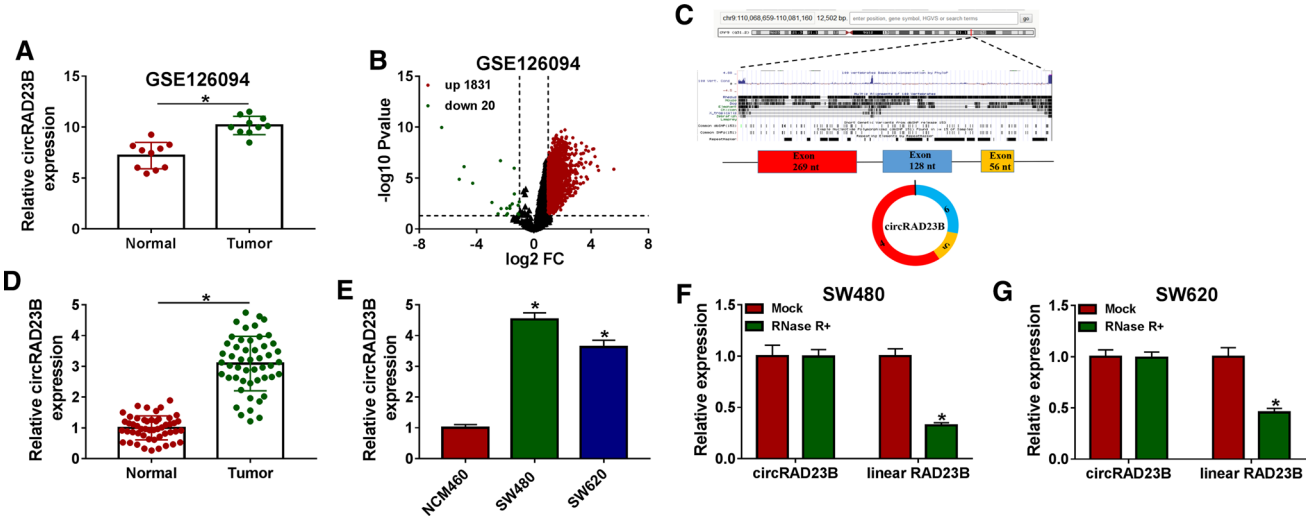

Fig. 1 CircRAD23B was highly expressed in CRC tissues and cells. **a**, **b** CircRAD23B expression (**a**) and dysregulated circRNAs (**b**) in CRC samples in GSE126094 dataset. (**c**) The genetic information of circRAD23B in the parental gene RAD23B. **d**, **e** The detection of circRAD23B in CRC tissues (**d**) and cells (**e**) was completed by qRT-PCR. **f**, **g** CircRAD23B and linear RAD23B levels were determined using qRT-PCR in SW480 and SW620 cells. All experiments were performed three times (N = 3). *$P < 0.05$

relative to Normal tissues and NCM460 cell line (Fig. 1d, e). Clinicopathologic features indicated that high circRAD23B expression was related to tumor TNM stage ($P = 0.004$) and tumor metastasis ($P = 0.023$) in CRC patients (Table 1). Besides, circRAD23B was more resistant to exonuclease RNase R than linear RAD23B in SW480 and SW620 cells (Fig. 1f, g), showing the stability of circRAD23B as a circRNA. Thus, circRAD23B was abnormally upregulated in CRC.

Downregulating circRAD23B Inhibited the Cancer Progression in CRC Cells

The interference of circRAD23B was achieved by siRNA transfection as illustrated in Fig. 2a, b, circRAD23B level was much lower in siRNA groups (si-circRAD23B#1, si-circRAD23B#2, si-circRAD23B#3) than that in si-NC group. We then performed the functional analysis of circRAD23B via exploring the effects of si-circRAD23B#2 (with more significant knockdown efficiency) on various cellular behaviors. An inhibitory phenomenon of cell

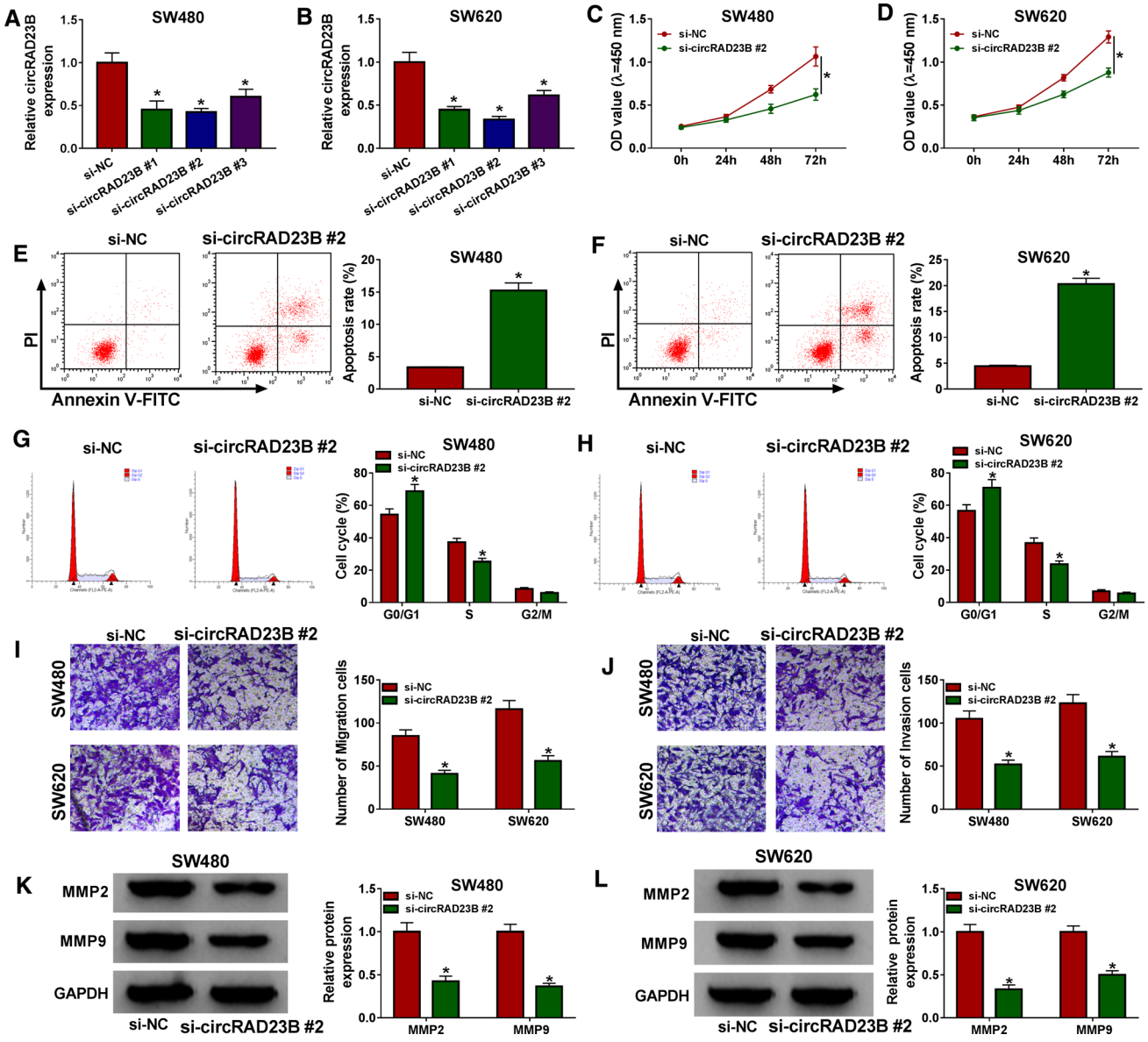

Fig. 2 Downregulating circRAD23B inhibited the cancer progression in CRC cells. **a**, **b** The qRT-PCR was administrated to examine circRAD23B expression in SW480 and SW620 cells transfected with si-NC or si-circRAD23B#2. **c**, **d** The proliferative abilities of the above transfected cells were analyzed via CCK-8 assay. **e**–**h** Flow cytometry was employed for the measurement of cell apoptosis (**e**, **f**) and cell cycle (**g**, **h**). **i**, **j** Transwell assay was performed to assess cell migration (**i**) and invasion (**j**). **k**, **l** The protein levels of MMP2 and MMP9 were assayed by western blot. All experiments were performed three times (N = 3). *$P < 0.05$

proliferation in CCK-8 assay (Fig. 2c, d) and a promoting effect on cell apoptosis in flow cytometry (Fig. 2e, f) were caused in SW480 and SW620 cells, as the consequences of circRAD23B downregulation. Additionally, knockdown of circRAD23B was shown to elevate cell distribution of G0/G1 phase and decrease that of S phase (with no difference of G2/M phase), resulting in the retardation of cell cycle (Fig. 2g, h). Transwell assay demonstrated that the migratory ability (Fig. 2i) and invasive potential (Fig. 2j) were reduced in si-circRAD23B#2-trasnfetced SW480 and SW620 cells compared to si-NC-transfected cells. Also, the invasion-related MMP2 and MMP9 protein levels were found to be repressed with the knockdown of circRAD23B (Fig. 2k, l). Altogether, CRC progression was inhibited by the downregulation of circRAD23B in vitro.

CircRAD23B Sponged miR-1205 in CRC Cells

After the target prediction by circinteractome and circBank and Venn diagram analysis, four miRNAs (miR-1205, miR-1253, miR-892b, miR-935) were screened as the candidate targets of circRAD23B. The qRT-PCR indicated that only miR-1205 expression was affected by si-circRAD23B#2 with 2.5-fold increase and we then chose miR-1205 as a target subject for circRAD23B (Supplementary Fig. 1). To analyze the effects of circRAD23B on miR-1205 level in CRC, SW480 and SW620 cells were transfected with si-NC or si-circRAD23B#2 and pcirc or circRAD23B. The qRT-PCR result displayed that silencing circRAD23B upregulated the expression of miR-1205 (Fig. 3a, b), and it was opposite that miR-1205 was downregulated by circRAD23B overexpression (Fig. 3c, d). The online circBank exhibited the binding sites for miR-1205 in the sequence of circRAD23B (Fig. 3e). Dual-luciferase reporter assay further manifested that miR-1205 mimic led to the luciferase inhibition in circRAD23B WT plasmid and no change was observed in circRAD23B MUT group (Fig. 3f, g), which affirmed the binding between circRAD23B and miR-1205. The miR-1205 expression was much lower in CRC tissues (Fig. 3h) and cells (Fig. 3i) by comparison with control tissues and cells. All these data showed that circRAD23B could generate the sponge effect on miR-1205 in CRC cells.

Upregulation of miR-1205 Was Answerable for the si-circRAD23B#2-Mediated Inhibition in CRC Development

Based on the transfection of si-circRAD23B#2, anti-miR-1205 was introduced into SW480 and SW620 cells with anti-miR-NC as the negative control for the mechanism analysis of circRAD23B. As the qRT-PCR data in Fig. 4a, b, the miR-1205 expression was decreased in si-circRAD23B#2 + anti-miR-1205 group contrasted with si-circRAD23B#2 + anti-miR-NC group, hinting that anti-miR-1205 transfection greatly inhibited miR-1205 in CRC cells. Subsequently, the si-circRAD23B#2-induced proliferation suppression (Fig. 4c, d), apoptosis promotion (Fig. 4e, f), and cell cycle arrest (Fig. 4g, h) were found to be

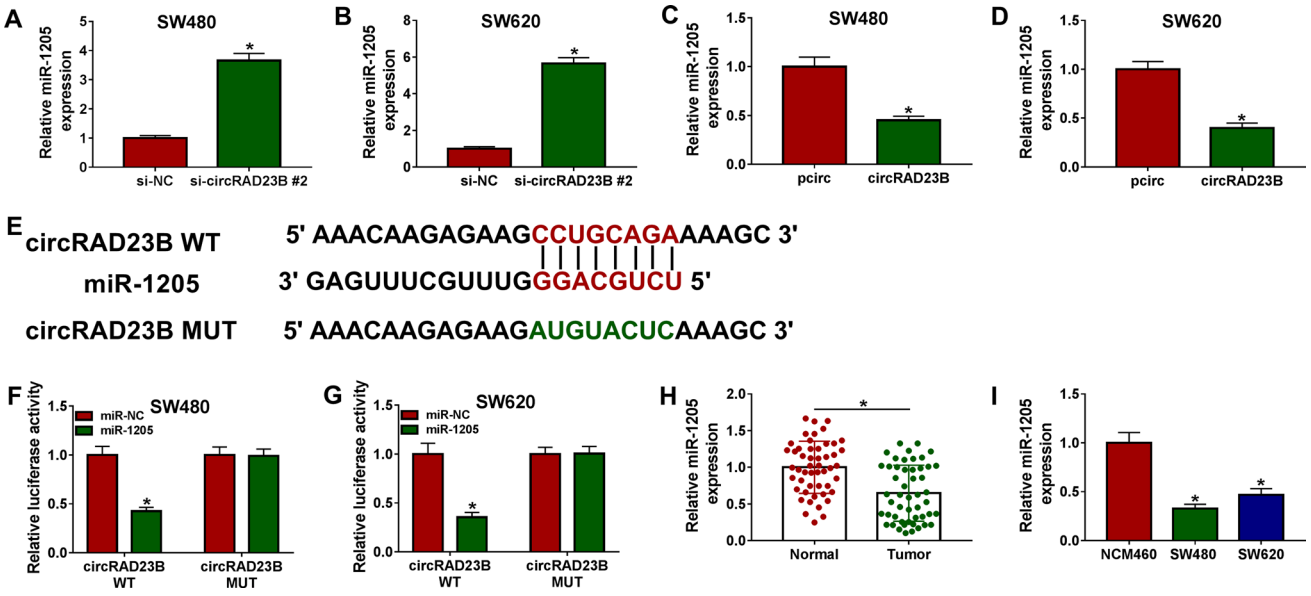

Fig. 3 CircRAD23B sponged miR-1205 in CRC cells. **a**–**d** The effects of circRAD23B downregulation (**a**, **b**) or overexpression (**c**, **d** on miR-1205 expression were detected applying with qRT-PCR. **e**–**g** The binding between circRAD23B and miR-1205 was predicted via circBank (**e**) and affirmed by dual-luciferase reporter assay (**f**, **g**). **h**, **i** The expression analysis of miR-1205 in CRC tissues (**h**) and cells (**i**) was carried out through the conduction of qRT-PCR. All experiments were performed three times (N = 3). *$P < 0.05$

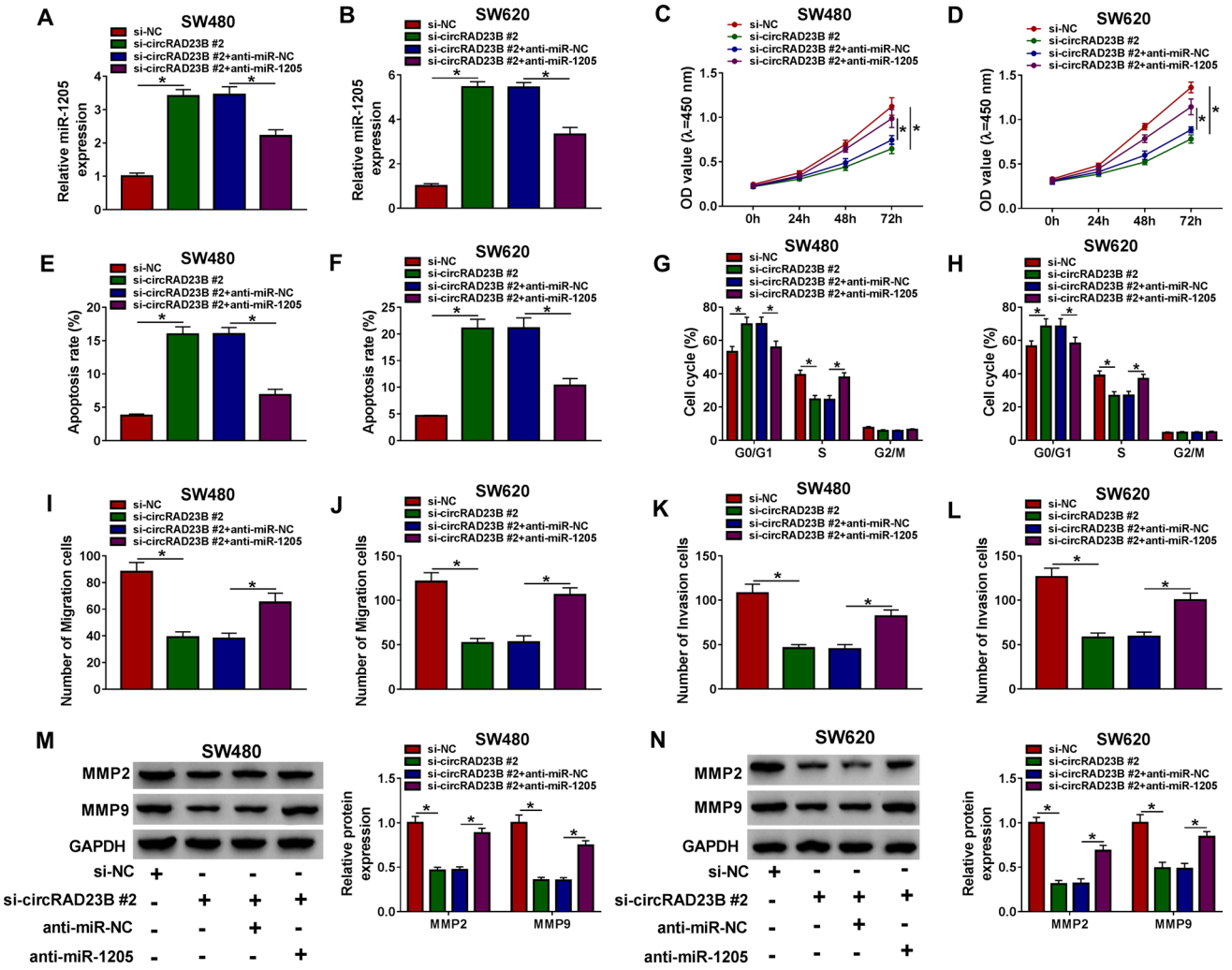

Fig. 4 Upregulation of miR-1205 was answerable for the si-circRAD23B#2-mediated inhibition in CRC development. **a**, **b** After SW480 and SW620 cells were transfected with si-NC, si-circRAD23B#2, si-circRAD23B#2 + anti-miR-NC or si-circRAD23B#2 + anti-miR-1205, miR-1205 was measured via qRT-PCR. **c**, **d** Cell proliferation analysis was implemented by CCK-8 assay. **e**–**h** Flow cytometry was used to evaluate the effects of above transfection on cell apoptosis (**e**, **f**) and cell cycle (**g**, **h**). **i**–**n** Cell metastasis was assessed by transwell assay for cell migration (**i, j**) and invasion (**k**, **l**) and western blot for MMP2 and MMP9 detection (**m**, **n**). All experiments were performed three times (N = 3). $^*P < 0.05$

countervailed by miR-1205 inhibitor. Similarly, the repressive effects on cell migration (Fig. 4i, j), invasion (Fig. 4k, l), and MMP2/MMP9 protein levels (Fig. 4m, n) triggered by si-circRAD23B#2 were also mitigated following the expression downregulation of miR-1205. Altogether, the downregulation of circRAD23B inhibited CRC progression via upregulating miR-1205.

MiR-1205 Negatively Regulated TRIM44 in CRC Cells

TRIM44 was shown to be upregulated in colon adenocarcinoma according to the dataset (Supplementary Fig. 2), and TargetScan software has presented the binding sites between miR-1205 and TRIM44 (Fig. 5a), implying the potential of TRIM44 as a target of miR-1205. Their interaction was verified using dual-luciferase reporter assay, in which only cotransfection of miR-1205 and TRIM44 3′UTR WT evoked the inhibition of luciferase activity (Fig. 5b, c). Pull-down assay also showed that the abundant TRIM44 was caught in Bio-miR-1205 group by contrast to Bio-miR-NC group (Fig. 5d, e). The qRT-PCR and western blot indicated that miR-1205 overexpression had inhibitory effect on the expression of TRIM44 in SW480 and SW620 cells (Fig. 5f, g). TRIM44 mRNA and protein levels were obviously elevated in CRC tissues (Fig. 5h, i) and cell (Fig. 5j, k) compared with their control groups. Therefore, TRIM44 was a downstream target of miR-1205 and was negatively regulated by miR-1205 in CRC cells.

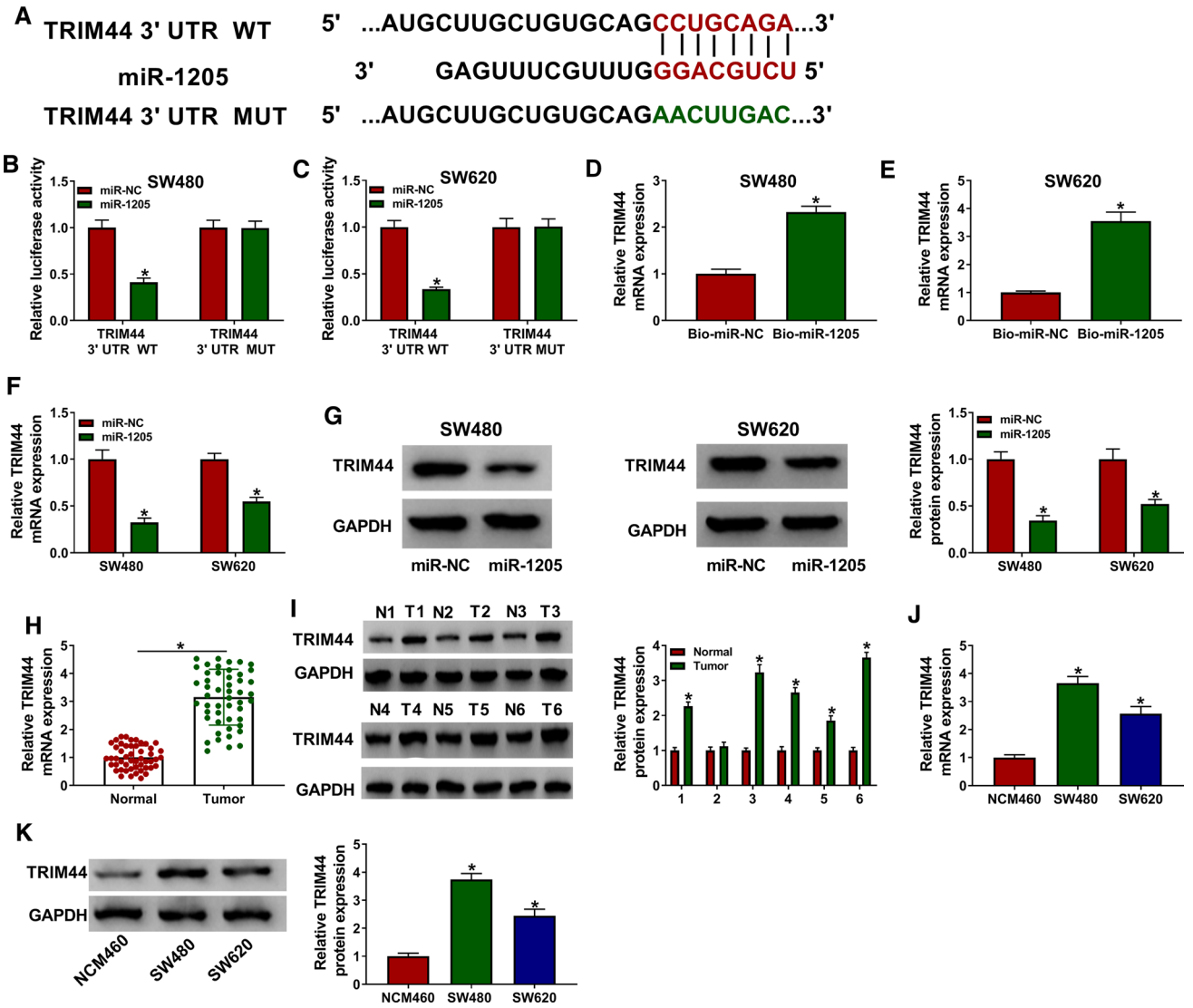

Fig. 5 MiR-1205 negatively regulated TRIM44 in CRC cells. a TargetScan was used for the target prediction of miR-1205. **b**–**e** Dual-luciferase reporter (**b**, **c**) and RNA pull-down (**d**, **e**) assays were performed to prove the combination of miR-1205 with TRIM44 in SW480 and SW620 cells. **f**, **g** TRIM44 mRNA and protein levels were assayed by qRT-PCR and western blot after respective transfection of miR-NC and miR-1205. **h**–**k** The qRT-PCR and western blot were exploited for TRIM44 level analysis in CRC tissues (**h**, **i**) and cells (**j**, **k**). All experiments were performed three times (N = 3). $^{*}P < 0.05$

MiR-1205 Downregulated TRIM44 to Function as a Tumor Inhibitor in CRC Cells

Transfection of miR-NC, miR-1205, miR-1205 + vector, and miR-1205 + TRIM44 was performed in SW480 and SW620 cells for the regulatory analysis between miR-1205 and TRIM44. Western blot exhibited that TRIM44 vector eliminated the inhibitory influence of miR-1205 on TRIM44 protein expression, affirming the great overexpression efficiency of TRMI44 transfection (Fig. 6a, b). Apparently, miR-1205 overexpression incurred the repression of proliferative capacity (Fig. 6c, d), acceleration of apoptotic generation (Fig. 6e, f), and the blockage of cell cycle progression (Fig. 6g, h), which were then ameliorated by the high TRIM44 expression in SW480 and SW620 cells. Also, TRIM44 upregulation restored the miR-1205-motivated suppressive effects on cell migration (Fig. 6i), invasion (Fig. 6j), and MMP2/MMP9 protein expression (Fig. 6k, l). As above described, miR-1205 played an inhibitory role in CRC via targeting TRIM44.

CircRAD23B Up-Modulated TRIM44 as a Sponge of miR-1205 in CRC Cells

To investigate whether circRAD23B could regulate TRIM44 via miR-1205, we transfected si-circRAD23B#2,

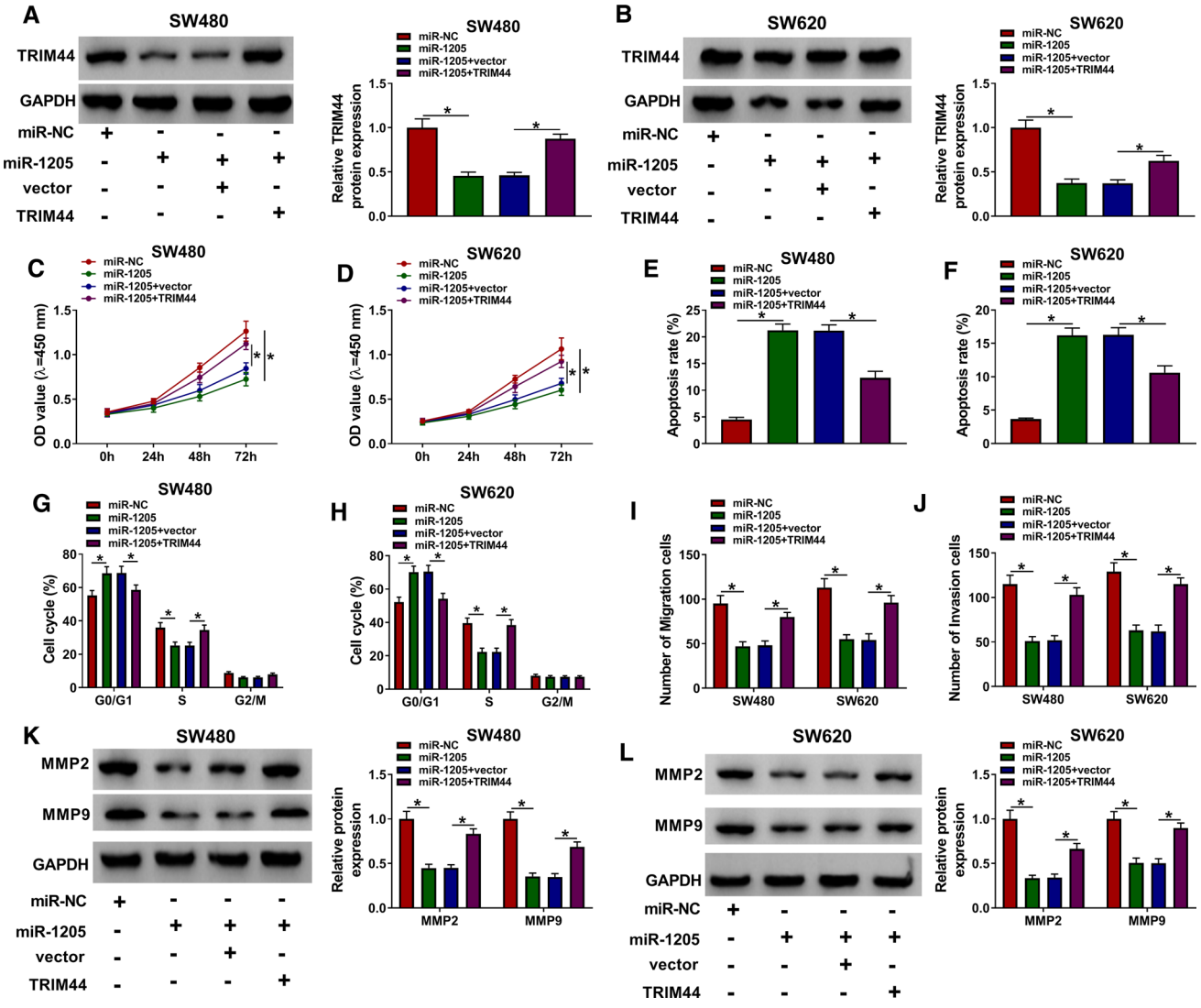

Fig. 6 MiR-1205 downregulated TRIM44 to function as a tumor inhibitor in CRC cells. **a**, **b** Western blot was performed for detecting TRIM44 protein expression in miR-NC, miR-1205, miR-1205 + vector, and miR-1205 + TRIM44 transfection groups. **c**, **d** CCK-8 assay was applied to determine cell proliferation. **e**–**h** cell apoptosis (**e**, **f**) and cell cycle (**g**, **h**) were examined by flow cytometry. **i**–**l** Cell migration (**i**) and invasion (**i**) by transwell assay together with MMP2 and MMP9 detection by western blot (**k**, **l**) were conducted to evaluate cell metastasis. All experiments were performed three times (N = 3). $^{*}P < 0.05$

si-circRAD23B#2 + anti-miR-1205, and the corresponding controls into SW480 and SW620 cells. The qRT-PCR analysis suggested that TRIM44 mRNA level was downregulated after transfection of si-circRAD23B#2, whereas there was a reversal for this downregulation by miR-1205 inhibitor (Fig. 7a, b). The same phenomenon was found in the protein expression of TRIM44 (Fig. 7c), again demonstrating the positive regulation of circRAD23B on TRIM44 by targeting miR-1205.

CRC Tumor Growth In Vivo Was Decelerated by circRAD23B Downregulation via the miR-1205/TRIM44 Network

After cell injection for 28 days in mice, tumor volume and weight of sh-circRAD23B group were exhibited to be declined in comparison with sh-NC group (Fig. 8a, b). The qRT-PCR and western blot were carried out for the expression analysis of three molecules in excised tumors. Sh-circRAD23B

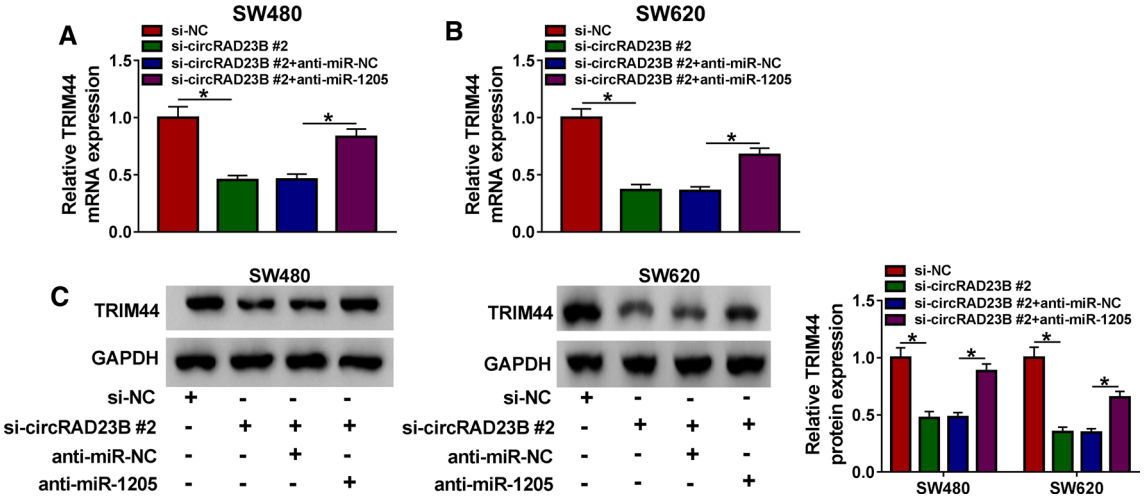

Fig. 7 CircRAD23B upmodulated TRIM44 as a sponge of miR-1205 in CRC cells. **a**–**c** TRIM44 mRNA (**a**, **b**) and protein (**c**) levels were, respectively, measured via qRT-PCR and western blot after si-circRAD23B#2, si-circRAD23B#2 + anti-miR-1205, or matched control transfection. All experiments were performed three times (N = 3). *$P < 0.05$

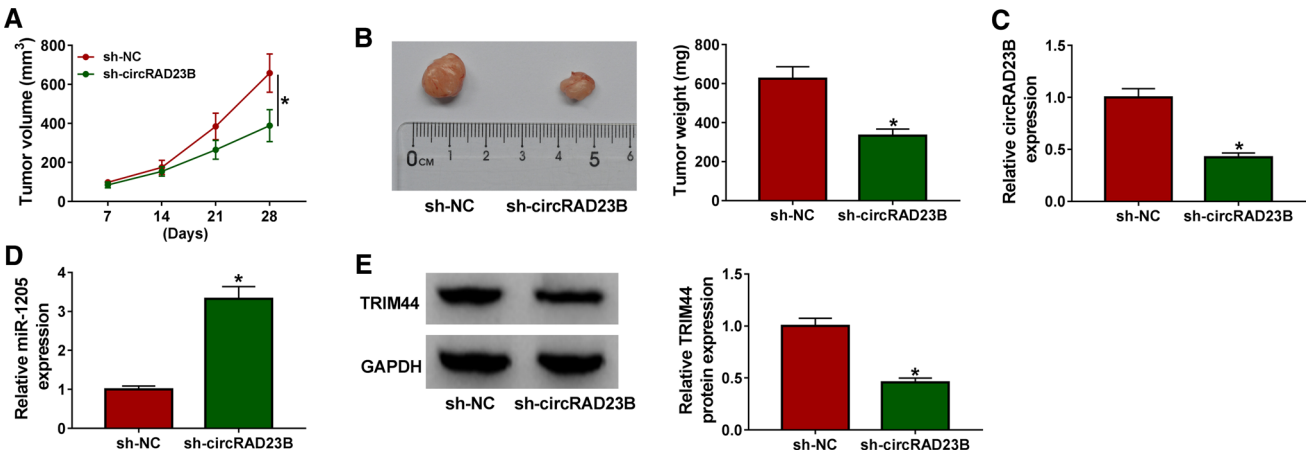

Fig. 8 CRC tumor growth in vivo was decelerated by circRAD23B downregulation via the miR-1205/TRIM44 network. **a** After the injection of SW480 cells transfected with sh-NC or sh-circRAD23B, the volume of tumor was measured every 7 days. **b** Tumors were weighed after 28 days. **c**–**e** The expression analysis was performed using qRT-PCR for circRAD23B (**c**) and miR-1205 (**d**), as well as western blot for TRIM44 (**e**). All experiments were performed three times (N = 3). *$P < 0.05$

introduction reduced the circRAD23B level (Fig. 8c) and enhanced miR-1205 expression (Fig. 8d) in tumors relative to sh-NC, indicating that knockdown of circRAD23B increased the level of its target miR-1205. This downregulation of circRAD23B in vivo also repressed TRIM44 protein expression (Fig. 8e). CRC tumorigenesis in vivo was also suppressed by circRAD23B inhibition by acting on the miR-1205/TRIM44 axis.

Discussion

Recently, circRNAs have become a research emphasis in different kinds of cancers due to their multitudinous characteristics of abundance, stability, and conservation in cancer cells [16]. CircRNA dysregulation has pivotal applications in the biomedical development [17].

For instance, hsa_circRNA_102958 upregulation was affirmed as a diagnostic indication for gastric cancer [18], and hsa_circ_000449 knockdown or overexpression significantly affected cell migratory and invasive abilities in oral squamous cell carcinoma [19]. Luo et al. proposed that circPTPRM was overexpressed in hepatocellular carcinoma and generated the promoting effects on tumorigenesis and metastasis [20]. Hou et al. showed that circASS1 was downregulated in breast cancer and retarded cell migration and invasion [21]. Additionally, increasing studies have reported many tumor-regulatory circRNAs in CRC, such as tumorigenic circVAPA/circBANP [22, 23] and suppressive circDDX17/circITGA7 [24, 25].

In the current study, circRAD23B was identified as an upregulated molecule in CRC tissue samples and cells compared with the relative control tissues and cells. CircRAD23B was more stable than linear RAD23B after the treatment of RNase R in CRC cells. Our cellular experiments further demonstrated that the low expression of circRAD23B induced the inhibition of CRC cell proliferation, cell cycle progression, cell migration and invasion along with the increased cell apoptosis. These results supported that circRAD23B downregulation motivated the antitumor response in CRC developing process.

CircRNAs have the sponge effects on miRNAs via the molecular interaction [26–28]. Intriguingly, we found that circRAD23B exerted the negatively regulatory influences on miR-1205 in CRC cells. Bioinformatic analysis and dual-luciferase reporter assay revealed the binding between circRAD23B and miR-1205. Moreover, circRAD23B was suggested to act in CRC cells depending on its sponge function for miR-1205. MiR-1205 is a regulatory molecule with antitumor response in laryngeal squamous cell carcinoma via targeting E2F1 [29] and in glioma via inhibiting BATF3 [30]. In addition to the identification of CRKL as a downstream gene for miR-1205 in CRC [12], the other targets of miR-1205 remain to be discovered. Herein, miR-1205 was able to target TRIM44 and directly repressed the expression of TRIM44 in CRC cells. Moreover, the reverted assays revealed that miR-1205 played as an inhibitor in the progression of CRC by downregulating TRIM44.

TRIM44 has been considered as a carcinogen in many common cancers, including renal cell carcinoma [31], glioma [32], cervical cancer [33], and CRC [13]. Ji et al. asserted that long ncRNA DUXAP8 facilitated nonsmall cell lung cancer development via upregulating TRIM44 by modulating miR-498 [34]. Sun et al. clarified that LINC00265 activated the glycolytic process of CRC through the miR-216b-5p/TRIM44 axis [35]. The regulation of circRNA on TRIM44 is unreported in previous studies. In this chapter, circRAD23B was proved to regulate TRIM44 in a positive manner via targeting miR-1205, exhibiting the circRAD23B/miR-1205/TRIM44 signal axis in CRC. The further in vivo experiments again confirmed that the downregulation of circRAD23B repressed tumor growth via the modulation of miR-1205/TRIM44 axis.

Conclusion

Taken together, all these results manifested that knockdown of circRAD23B targeted the miR-1205/TRIM44 axis to suppress the progression of CRC. CircRAD23B can be used as a reliable target for CRC diagnosis, and circRAD23B inhibition may contribute to the therapeutic development of CRC as an effective antitumor option.

Supplementary Information The online version of this article (https://doi.org/10.1007/s10620-021-06859-w) contains supplementary material, which is available to authorized users.

Funding No funding was received.

Compliance with Ethical Standards

Conflict of interest The authors declare that they have no conflict of interest.

References

1. Wang W, Kandimalla R, Huang H et al. Molecular subtyping of colorectal cancer: recent progress, new challenges and emerging opportunities. *Semin Cancer Biol.* 2019;55:37–52. https://doi.org/10.1016/j.semcancer.2018.05.002.
2. Pang SW, Awi NJ, Armon S et al. Current update of laboratory molecular diagnostics advancement in management of colorectal cancer (CRC). *Diagnostics (Basel)* 2019;10:9. https://doi.org/10.3390/diagnostics10010009.
3. Mei XL, Zheng QF. Role of cellular biomolecules in screening, diagnosis and treatment of colorectal cancer. *Curr Drug Metab.* 2019;20:880–888. https://doi.org/10.2174/1389200220666191018153428.
4. Wang P, He X. Current research on circular RNAs associated with colorectal cancer. *Scand J Gastroenterol.* 2017;52:1203–1210. https://doi.org/10.1080/00365521.2017.1365168.
5. Mumtaz PT, Taban Q, Dar MA et al. Deep insights in circular RNAs: from biogenesis to therapeutics. *Biol Proced Online* 2020;22:10. https://doi.org/10.1186/s12575-020-00122-8.
6. Lu C, Fu L, Qian X et al. Knockdown of circular RNA circFARSA restricts colorectal cancer cell growth through regulation of miR-330-5p/LASP1 axis. *Arch Biochem Biophys.* 2020;689:108434. https://doi.org/10.1016/j.abb.2020.108434.
7. Yin W, Xu J, Li C et al. Circular RNA circ_0007142 facilitates colorectal cancer progression by modulating CDC25A expression via miR-122-5p. *Onco Targets Ther.* 2020;13:3689–3701. https://doi.org/10.2147/OTT.S238338.
8. Wang J, Luo J, Liu G et al. Circular RNA hsa_circ_0008285 inhibits colorectal cancer cell proliferation and migration via the miR-382-5p/PTEN axis. *Biochem Biophys Res Commun.* 2020;527:503–510. https://doi.org/10.1016/j.bbrc.2020.03.165.

9. Braicu C, Zimta AA, Harangus A et al. The function of non-coding RNAs in lung cancer tumorigenesis. *Cancers (Basel)* 2019;11:605. https://doi.org/10.3390/cancers11050605.
10. Lan X, Liu X, Sun J et al. CircRAD23B facilitates proliferation and invasion of esophageal cancer cells by sponging miR-5095. *Biochem Biophys Res Commun.* 2019;516:357–364. https://doi.org/10.1016/j.bbrc.2019.06.044.
11. Han W, Wang L, Zhang L et al. Circular RNA circ-RAD23B promotes cell growth and invasion by miR-593-3p/CCND2 and miR-653-5p/TIAM1 pathways in non-small cell lung cancer. *Biochem Biophys Res Commun.* 2019;510:462–466. https://doi.org/10.1016/j.bbrc.2019.01.131.
12. Jiang Y, Liu G, Ye W et al. ZEB2-AS1 accelerates epithelial/mesenchymal transition through miR-1205/CRKL pathway in colorectal cancer. *Cancer Biother Radiopharm.* 2020;35:153–162. https://doi.org/10.1089/cbr.2019.3000.
13. Li CG, Hu H, Yang XJ et al. TRIM44 promotes colorectal cancer proliferation, migration, and invasion through the Akt/mTOR signaling pathway. *Onco Targets Ther.* 2019;12:10693–10701. https://doi.org/10.2147/OTT.S228637.
14. Lei R, Feng L, Hong D. ELFN1-AS1 accelerates the proliferation and migration of colorectal cancer via regulation of miR-4644/TRIM44 axis. *Cancer Biomark.* 2020;27:433–443. https://doi.org/10.3233/CBM-190559.
15. Gu J, Xu T, Huang QH et al. HMGB3 silence inhibits breast cancer cell proliferation and tumor growth by interacting with hypoxia-inducible factor 1alpha. *Cancer Manag Res.* 2019;11:5075–5089. https://doi.org/10.2147/CMAR.S204357.
16. Tang Q, Hann SS. Biological roles and mechanisms of circular RNA in human cancers. *Onco Targets Ther.* 2020;13:2067–2092. https://doi.org/10.2147/OTT.S233672.
17. Holdt LM, Kohlmaier A, Teupser D. Molecular roles and function of circular RNAs in eukaryotic cells. *Cell Mol Life Sci.* 2018;75:1071–1098. https://doi.org/10.1007/s00018-017-2688-5.
18. Wei J, Wei W, Xu H et al. Circular RNA hsa_circRNA_102958 may serve as a diagnostic marker for gastric cancer. *Cancer Biomark.* 2020;27:139–145. https://doi.org/10.3233/CBM-182029.
19. Li X, Zhang H, Wang Y et al. Silencing circular RNA hsa_circ_0004491 promotes metastasis of oral squamous cell carcinoma. *Life Sci.* 2019;239:116883. https://doi.org/10.1016/j.lfs.2019.116883.
20. Luo Z, Mao X, Cui W. Circular RNA expression and circPTPRM promotes proliferation and migration in hepatocellular carcinoma. *Med Oncol.* 2019;36:86. https://doi.org/10.1007/s12032-019-1311-z.
21. Hou JC, Xu Z, Zhong SL et al. Circular RNA circASS1 is down-regulated in breast cancer cells MDA-MB-231 and suppressed invasion and migration. *Epigenomics* 2019;11:199–213. https://doi.org/10.2217/epi-2017-0167.
22. Li XN, Wang ZJ, Ye CX et al. Circular RNA circVAPA is up-regulated and exerts oncogenic properties by sponging miR-101 in colorectal cancer. *Biomed Pharmacother.* 2019;112:108611. https://doi.org/10.1016/j.biopha.2019.108611.
23. Zhu M, Xu Y, Chen Y et al. Circular BANP, an upregulated circular RNA that modulates cell proliferation in colorectal cancer. *Biomed Pharmacother.* 2017;88:138–144. https://doi.org/10.1016/j.biopha.2016.12.097.
24. Li XN, Wang ZJ, Ye CX et al. RNA sequencing reveals the expression profiles of circRNA and indicates that circDDX17 acts as a tumor suppressor in colorectal cancer. *J Exp Clin Cancer Res.* 2018;37:325. https://doi.org/10.1186/s13046-018-1006-x.
25. Li X, Wang J, Zhang C et al. Circular RNA circITGA7 inhibits colorectal cancer growth and metastasis by modulating the Ras pathway and upregulating transcription of its host gene ITGA7. *J Pathol.* 2018;246:166–179. https://doi.org/10.1002/path.5125.
26. Jin Y, Yu LL, Zhang B et al. Circular RNA hsa_circ_0000523 regulates the proliferation and apoptosis of colorectal cancer cells as miRNA sponge. *Braz J Med Biol Res.* 2018;51:e7811. https://doi.org/10.1590/1414-431X20187811.
27. Yuan Y, Liu W, Zhang Y et al. CircRNA circ_0026344 as a prognostic biomarker suppresses colorectal cancer progression via microRNA-21 and microRNA-31. *Biochem Biophys Res Commun.* 2018;503:870–875. https://doi.org/10.1016/j.bbrc.2018.06.089.
28. Qiu L, Huang Y, Li Z et al. Circular RNA profiling identifies circADAMTS13 as a miR-484 sponge which suppresses cell proliferation in hepatocellular carcinoma. *Mol Oncol.* 2019;13:441–455. https://doi.org/10.1002/1878-0261.12424.
29. Li P, Lin XJ, Yang Y et al. Reciprocal regulation of miR-1205 and E2F1 modulates progression of laryngeal squamous cell carcinoma. *Cell Death Dis.* 2019;10:916. https://doi.org/10.1038/s41419-019-2154-4.
30. Yi C, Li H, Li D et al. Upregulation of circular RNA circ_0034642 indicates unfavorable prognosis in glioma and facilitates cell proliferation and invasion via the miR-1205/BATF3 axis. *J Cell Biochem.* 2019;120:13737–13744. https://doi.org/10.1002/jcb.28646.
31. Yamada Y, Kimura N, Takayama KI et al. TRIM44 promotes cell proliferation and migration by inhibiting FRK in renal cell carcinoma. *Cancer Sci.* 2020;111:881–890. https://doi.org/10.1111/cas.14295.
32. Zhou X, Yang Y, Ma P et al. TRIM44 is indispensable for glioma cell proliferation and cell cycle progression through AKT/p21/p27 signaling pathway. *J Neurooncol.* 2019;145:211–222. https://doi.org/10.1007/s11060-019-03301-0.
33. Liu S, Meng F, Ding J et al. High TRIM44 expression as a valuable biomarker for diagnosis and prognosis in cervical cancer. *Biosci Rep.* 2019;39:20181639. https://doi.org/10.1042/BSR20181639.
34. Ji X, Tao R, Sun LY et al. Down-regulation of long non-coding RNA DUXAP8 suppresses proliferation, metastasis and EMT by modulating miR-498 through TRIM44-mediated AKT/mTOR pathway in non-small-cell lung cancer. *Eur Rev Med Pharmacol Sci.* 2020;24:3152–3165. https://doi.org/10.26355/eurrev_202003_20682.
35. Sun S, Li W, Ma X et al. Long noncoding RNA LINC00265 promotes glycolysis and lactate production of colorectal cancer through regulating of miR-216b-5p/TRIM44 axis. *Digestion.* 2019. https://doi.org/10.1159/000500195.